Applied Nanoscience (2023) 13:4235–4245
https://doi.org/10.1007/s13204-023-02873-8

ORIGINAL ARTICLE

Cocoa pod shell mediated silver nanoparticles synthesis, characterization, and their application as nanocatalyst and antifungal agent

Vinayaka B. Shet[1] · P. Senthil Kumar[2,3,9,10] · Ramesh Vinayagam[4] · Raja Selvaraj[4] · C. Vibha[1] · Shravya Rao[1] · S. M. Pawan[1] · G. Poorvika[1] · Valentina Marmolejo Quintero[5] · P. Ujwal[1] · K. S. Rajesh[6] · Akhilesh Dubey[7] · Silvia Yumnam[8]

Received: 31 May 2022 / Accepted: 3 May 2023 / Published online: 10 May 2023
© King Abdulaziz City for Science and Technology 2023

Abstract

Cocoa pod shells are the byproducts of the cocoa industry. These pod shells were explored for the biogenic synthesis of silver nanoparticles. The synthesized nanoparticles were characterized, and studies were carried out to assess the catalytic and antifungal activities. UV–Vis spectral analysis recorded the surface plasmon resonance at 438 nm. Spherical-shaped particles with a diameter ranging from 48.83 to 55.24 nm were determined by scanning electron microscope. The presence of silver was confirmed through Energy Dispersive X-Ray Analysis. FTIR analysis was carried out to determine the functional groups capped on the surface of the nanoparticles. XRD patterns substantiated the crystalline nature with the sharp peak of 33.16° indicating (101) fcc plane and crystallite size were calculated to be 59.65 nm. Amylase activity was found to be sevenfold higher with a significant amount of 16.05 mg/ml/min in the presence of silver nanoparticles as compared to the control. Methylene blue dye degradation in the presence of silver nanoparticles followed a pseudo-first-order reaction with a degradation constant of 0.1889 min^{-1} and R^2 of 0.9869. In addition, an inhibition activity of 34% against *Fusarium oxysporum* f. sp. *cubense* fungi was exhibited by the synthesized silver nanoparticles. The outcome of the investigation has revealed the potential scope of silver nanoparticles as nanocatalysts in starch hydrolysis, dye degradation as well as the antifungal potential.

Keywords Cocoa pod shell · Silver nanocatalyst · Amylase activity · Starch hydrolysis · Antifungal activity

✉ Vinayaka B. Shet
vinayakabshet@nitte.edu.in

1 Department of Biotechnology Engineering, Nitte (Deemed to be University), NMAM Institute of Technology (NMAMIT), Nitte 574110, Karnataka, India

2 Department of Chemical Engineering, Sri Sivasubramaniya Nadar College of Engineering, Chennai 603110, India

3 Centre of Excellence in Water Research (CEWAR), Sri Sivasubramaniya Nadar College of Engineering, Chennai 603110, India

4 Department of Chemical Engineering, Manipal Institute of Technology, Manipal Academy of Higher Education, Udupi District, Manipal, Karnataka 576104, India

5 Facultad de Ciencias Agrarias, Politécnico Colombiano Jaime Isaza Cadavid, Medellín, Colombia

6 Department of Pharmacology, Nitte (Deemed to be University), NGSM Institute of Pharmaceutical Sciences, Paneer, Deralakatte, Mangaluru, Karnataka 575 018, India

7 Department of Pharmaceutics, Nitte (Deemed to be University), NGSM Institute of Pharmaceutical Sciences, Paneer, Deralakatte, Mangaluru, Karnataka 575 018, India

8 Institute of Bioresource and Sustainable Development, Imphal, Manipur 795001, India

9 School of Engineering, Lebanese American University, Byblos, Lebanon

10 Department of Biotechnology Engineering and Food Technology, Chandigarh University, Mohali 140413, India

Introduction

Nanotechnology is an emerging field of modern research dealing with the synthesis, application, and tailoring of particle structures that exist in the nano regime. Currently, nanoparticles are gaining importance due to their promising role in building blocks as well as applications in various elements of utilization. Though there exists a broad range of methods for the synthesis of nanoparticles, novel nanoparticles can be synthesized using an eco-friendly approach to avoid hazardous elements. The synthesis process is cost-effective, simple, and safe (Lateef et al. 2015), and this also provides an advantage of easy scale-up for large-scale synthesis. Biological molecules are explored to be implemented as capping and stabilizing components for biogenic nanoparticles (Varadavenkatesan et al. 2020a, b). These nanoparticles are synthesized by deploying roots, stems, leaves, flowers, fruits, seeds, and pods (Pai et al. 2019; Anchan et al. 2019). Furthermore, due to the potential usage of nanoparticles in a wide range of products, the synthesis of nanoparticles can be explored in the agro-waste thereby enhancing the sustainability and efficacy of the process.

Amylase enzyme has widespread commercial applications in the industry. To name a few, starch hydrolysis enzymes in the adhesive industry (Monroy et al. 2020), bioethanol production (Tong et al. 2019; Maia et al. 2020), textile industry (Ahmed and Kolisis 2011), and starch modifications (Wang et al. 2017) and many others. On the other hand, enhancing the catalytic potential of amylases using silver nanoparticles is also gaining importance (Halima and Narula 2019). Hence understanding the impact of silver nanoparticles on enhanced amylase activity will pave the way for exploring the applications in a wide array of the environment which includes agriculture, biofuels, pharmaceutical, food, medicine, and starch hydrolysis (Falkowska and Molga 2014; Krishnakumar et al. 2018; Thakur et al. 2022; Al-Buriahi et al. 2022; Assad et al. 2022; Vo et al. 2022).

The widespread distribution of the fungus *Fusarium oxysporum* f. sp. *Cubense* Race 4 (FocR4) is attributed to their ability to grow on a wide range of substrates and their efficient dispersal mechanisms. These are filamentous fungi that are widely distributed in soil, water, subterranean and aerial plant parts, and other substrates. It has been responsible for infecting and damaging a huge quantity of crops especially bananas (Dita et al. 2018). Though studies have been undertaken on antagonism property against FocR4, there remains a gap in the efficacy of the utilized sources (Yadav et al. 2021).

Cocoa (*Theobroma cacao*) is known as the key economic crop of Ghana. Only 25% of the total weight of cocoa fresh fruits is used for the production of cocoa beans for chocolate processing, wherein cocoa pod shells are discarded. The outer shell of cocoa is separated along with the germ after or before roasting and the broken fragments of cotyledon, called nibs without the shells are used in the production of chocolate. Cocoa pod shells (CPS) represent 70–75% (wt) of the cocoa fruits, hence each ton of the fruit generates 700–750 kg of agricultural residue (Cruz et al. 2012). The cocoa pod shell consists of gallic acid equivalent of soluble phenolic (45.6–46.4 mg), carbohydrate (32.3%), lignin (21.44%), sugars (19.2%), proteins (8.6%), and minerals (27.7%). CPS is abundantly accessible in the district of Dakshina Kannada in Karnataka state, India (Shet et al. 2018). Agro residue CPS is available abundantly. Disposal of CPS is challenging to farmers since it reduces the fertility of the soil. Hence channelizing CPS for a productive purpose is essential.

The present investigation navigates the first of its kind on CPS explored for biogenic silver nanoparticle synthesis. In the current investigation, the potential of the agro residue CPS was tapped to synthesize, characterize, and investigate the effect of silver nanoparticles on amylase activity, degradation of methylene dye, and antifungal activity. To the best of our knowledge, there have been no studies on the application of nanoparticles synthesized from cocoa pod shells on the inhibition against FocR4 as well.

Materials and methods

Collection and preparation of CPS

Cocoa pod shells were collected from Peruvai village, Bantwal taluk, Karnataka (Altitude: 89 m; Latitude: 12.710135; Longitude: 75.065417) India, and processed to obtain the powder. Sieving was carried out using mesh number 200; CPS powder was stored at 4 °C till further use (Shet et al. 2019). CPS extract was prepared by boiling 1 g of CPS powder in 100 ml of distilled water at 100 °C for 15 min using a water bath. Further, the solution was cooled to room temperature and filtered using Whatman filter paper to obtain a clear extract (Fig. 1).

Synthesis of silver nanoparticles

10 ml CPS extract was added to 100 ml silver nitrate solution (1 mM) and placed overnight in the shaker under dark conditions. The change in color from pale yellow to orange confirms the formation of silver nanoparticles. The interaction between silver ions in the solution and molecules present in the extract reduce silver ions to silver by capping on the surface (Fig. 2).

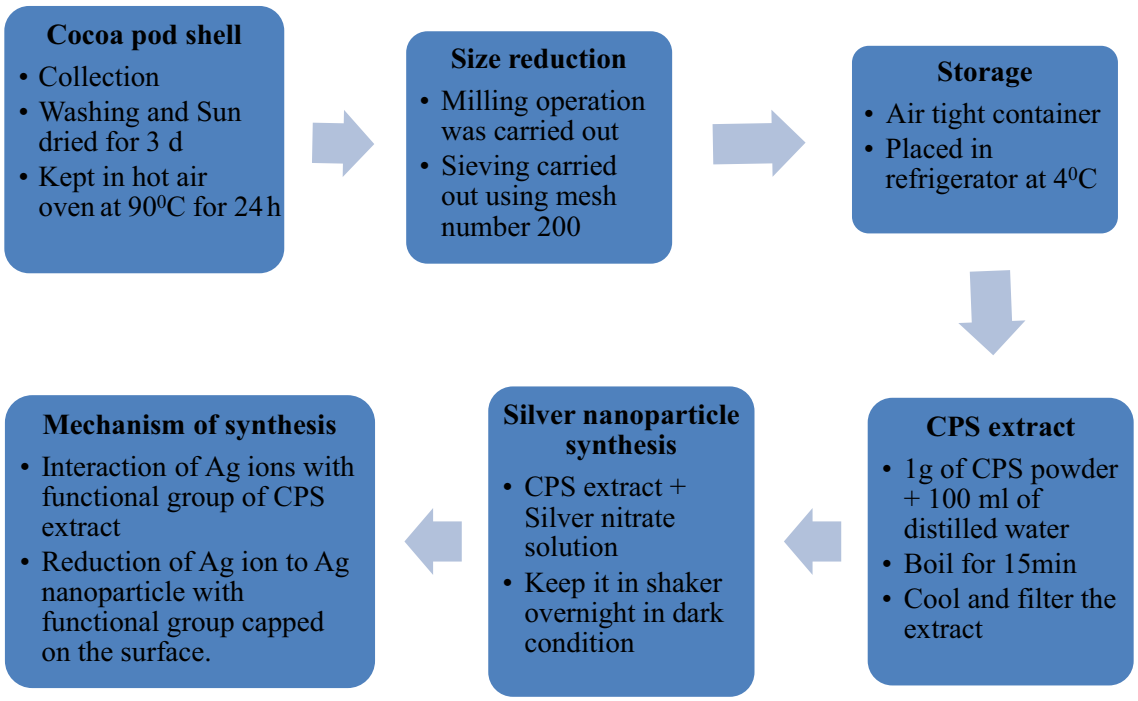

Fig. 1 Process flow chart for the preparation of CPS extract and Ag nanoparticle synthesis

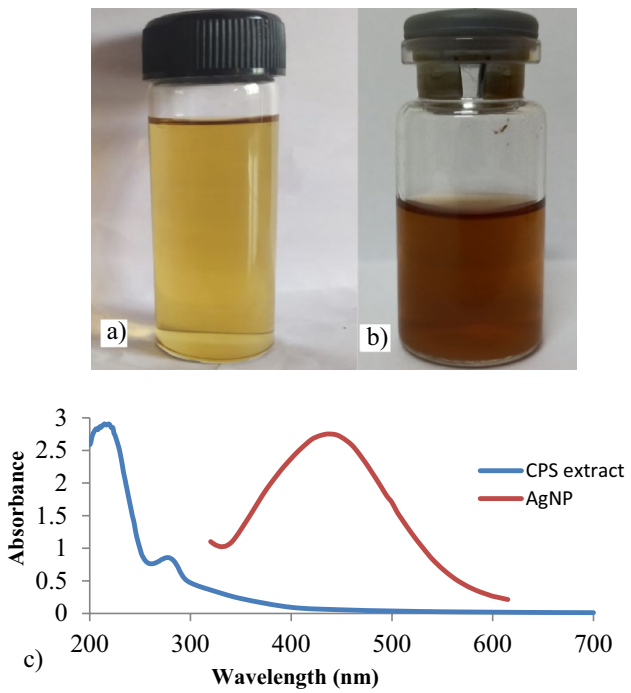

Fig. 2 **a** CPS extract **b** biogenic silver nanoparticle **c** UV Vis spectra of CPS extract and AgNPs

Characterization of nanoparticles

Silver nanoparticle solution was scanned using a UV–vis spectrophotometer between 350 to 700 nm to check the surface plasmon resonance (SPR) peak of the silver nanoparticles. The dynamic light scattering (DLS) method using Malvern Zeta Sizer (Malvern Instruments, Malvern, UK) was used to determine the particle size distribution. The particle size distribution and hydrodynamic diameter of particles were obtained directly from the instrument through CONTIN analysis. Fourier Transform Infrared Spectroscopy (FTIR) (Alpha Bruker, Japan) was adopted to determine the possible functional group capped on the silver nanoparticle and its bond stretching vibrations. The analysis was carried out between the wavenumbers 500 to 4000 cm^{-1}. Colloidal silver nanoparticles were placed on the glass slide and allowed to dry to determine the shape, size, and elemental composition of the nanoparticle using Field Emission Scanning Electron Microscope. Patterns obtained from the X-ray diffraction (XRD) analysis provided insight into the crystalline structure of the silver nanoparticles and its size.

Silver nanoparticle-mediated enzyme assay

The amylase enzyme assay was performed using commercially available fungal amylase enzyme procured from Molychem company. The test tubes containing enzyme (0.5 ml) and soluble starch in phosphate buffer (0.1 ml) were mixed

with the increasing volume of silver nanoparticles. Buffer was used to make up the volume to 3.5 ml. The assay was carried out in duplicates. A control reaction tube containing enzyme and substrate was maintained without silver nanoparticles to investigate the effect of nano-catalytic activity. The reaction containers were incubated at room temperature for 10 min. Dinitrosalicylic acid (DNSA) reagent of 1 ml was added to all the test tubes and kept in the thermostat for 10 min. The solution was allowed to cool and absorbance was measured at 540 nm using a spectrophotometer (Miller 1959). Amylase assay was performed following the DNSA method.

Assessment of dye degradation potential

Biosynthesized silver nanoparticle solution of 50 µL was treated with 2 mL of Methylene blue dye along with 50 µL of $NaBH_4$ in a cuvette. Negative control was used in a separate cuvette without silver nanoparticles. Contents were thoroughly mixed using a micropipette before scanning the sample using a UV–vis spectrophotometer between 400 and 700 nm. The absorbance value at 663 nm of the methylene blue dye was monitored for different intervals of time till the complete degradation occurred under static conditions (Vinayagam et al. 2017; Yadav et al. 2019).

Inhibition activity of silver nanoparticles against FocR4

Culturing of *Fusarium oxysporum* f. sp. *cubense* (FocR4)

FocR4 was obtained from Microbiology Research Laboratory, Kuvempu University, Shivamoga, Karnataka. The FocR4 was subcultured in the laboratory using Potato Dextrose Agar medium (PDA) and was further used in the studies.

Disc inhibition test against *Fusarium oxysporum* f. sp. *cubense* (FocR4)

The inhibition activity of synthesized nanoparticles was tested against FocR4. 5 days old FocR4 mycelium was taken from the culture plate for disc inhibition test throughout the experimental studies. This was carried out by placing a 0.5 cm FocR4 disc in the center of a Petri dish containing Nutritive Agar. A 0.5 cm sterile filter paper disc was taken using sterile forceps and was introduced into the Erlenmeyer with 5 ml of colloidal nanoparticle solution. This was further placed on the side of the FocR4 disc, at a distance of approximately 2 cm. Another similar set was maintained using the crude extract of cocoa pod shell extract on another Petri plate. To observe the normal growth of FocR4 (without inhibition), a disc was kept separately in a Petri plate in the center of the culture medium, which served as a control. The inoculated plate was incubated at 30 °C for 5 days and the zone of inhibition of FocR4 was measured using a Vernier caliper. The growth inhibition zone of the fungus was calculated using the below-given formulae:

$$\%\ Inhibition = \frac{FocR4C - FocR4B}{FocC} * 100$$

Where FocR4 C: FocR4 was taken as control. FocR4 B: FocR4 Vs Nanoparticles.

Results and discussion

SPR analysis

The synthesis of biogenic silver nanoparticles using CPS extract (Fig. 2a) as a reducing agent was performed at room temperature. The change of color to pale orange confirms the synthesis of nanoparticles. The UV visible spectrum of CPS extract is represented in Fig. 2c. Scanning the biogenic nanoparticle solution (Fig. 2b) using a UV Visible spectrophotometer between 350 and 700 nm reveals the characteristic SPR peak of silver nanoparticles at 438 nm (Fig. 2c). Spherical shaped silver nanoparticle exhibits SPR band in the range of 350 to 500 nm (Ider et al. 2017). Based on Mie's theory, a single symmetric SPR band indicates the presence of isotropic silver nanoparticles of spherical shape (Hao et al. 2004). The peaks observed in the range of 200 to 400 nm of the CPS extract endorses the existence of heteroatoms and unsaturated groups (Jain et al. 2016). These molecules were accountable for the reduction of silver ions and capped on the silver nanoparticles (Vinayagam et al. 2018; Varadavenkatesan et al. 2021).

Particle size distribution

The synthesis of biogenic silver nanoparticles was characterized by a zeta sizer to determine the average size and distribution pattern. The particle size ranges from approximately

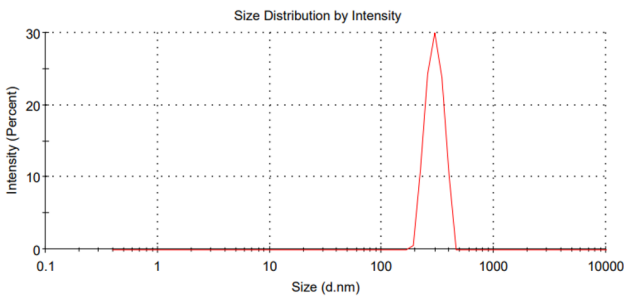

Fig. 3 Size distribution of biogenic silver nanoparticle

190 to 490 nm. The mean particle size was estimated at 384 nm (Fig. 3). The zeta potential value was measured to be − 13.7 mV. The value indicated the presence of a negative charge on the surface and the stability of the silver nanoparticles (Dhyani 2016).

Size, shape, and elemental composition

Biosynthesized silver nanoparticles were spherical with a diameter ranging from 48.83 to 55.24 nm (Fig. 4a). The appearance of aggregate formation is probably due to the sample preparation process involved in the analysis. The EDS analysis confirms the presence of silver atoms at 2.98 keV (Fig. 4b).

XRD

Crystalline structures of the biosynthesized silver nanoparticles were interpreted based on X-ray diffraction analysis (Fig. 5). Several peaks were observed at various 2θ (°) values such as 28.74, 33.16, 38.72, 45.14, 47.12, 65.12, and 68.13. The sharp peak of 33.16° indicates (101) fcc plane (JCPDS, File No. 04-0783), and the crystallite size was calculated as 59.65 nm. The d-spacing and lattice parameter

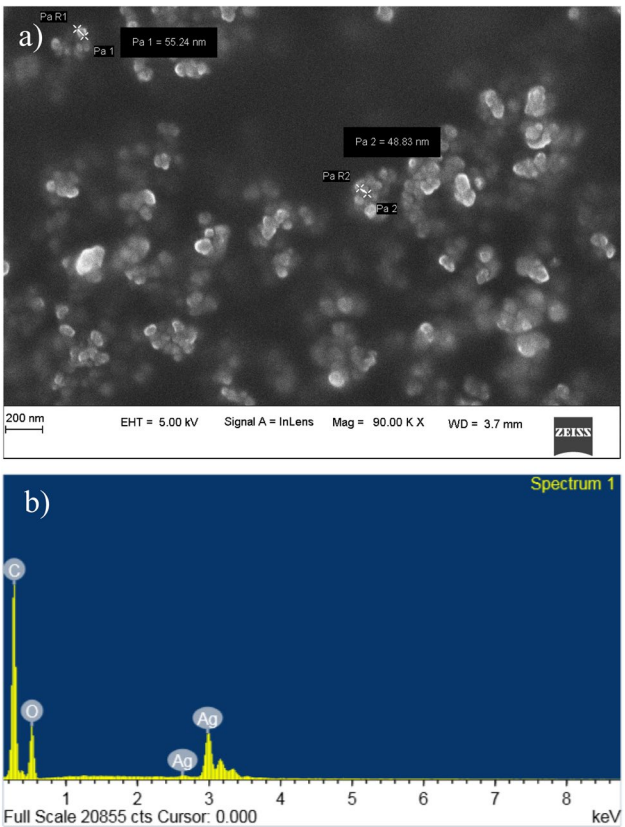

Fig. 4 **a** SEM image of biosynthesized silver nanoparticles **b** elemental composition of biosynthesized silver nanoparticles

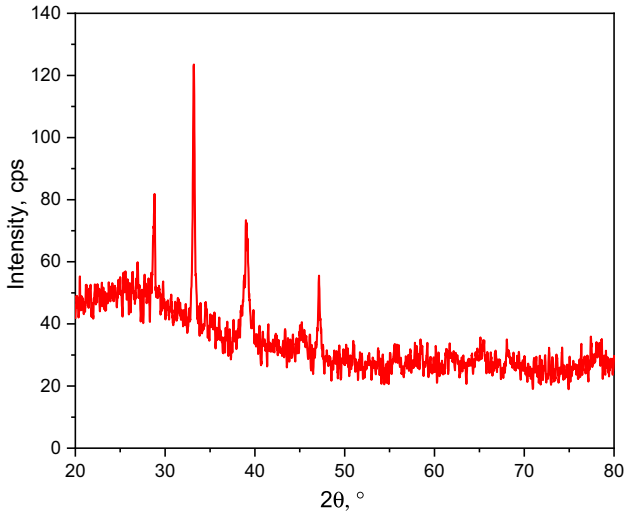

Fig. 5 XRD pattern of biosynthesized silver nanoparticle

values were determined as 0.26 nm and 0.38 nm respectively, which is consistent with the literature (Raja et al. 2015; Yadav et al. 2019).

Determination of functional groups

The functional groups present in the CPS extract responsible for reducing the silver ions and forming the capping agents were determined using FTIR. Superimposed spectral bands of FTIR for CPS extract and biogenic nanoparticles are depicted in Fig. 6. The bands represent the presence of different functional groups. Two absorption bands exhibited shifts 1634–1638 cm^{-1} (protein moiety with double bond corresponds to C = C stretch) and 3315–3340 cm^{-1} (O–H stretching) (Nandiyanto et al. 2019). Hence, it is evident that two functional moieties are capped onto the surface of silver nanoparticles. The shift asserts the role of alkene (Nguyen et al. 2020) and alcohols (Dewi et al. 2021) present in the CPS extract to reduce silver ions. Results of UV visible SPR spectra and FTIR bands prove the role of CPS extract in the synthesis of silver nanoparticles.

Mechanism of silver nanoparticle synthesis

Silver ions interact with functional groups present in the CPS extract. The peaks of CPS extract (Fig. 2c) endorse the presence of unsaturated groups and heteroatoms. Silver ions undergo reduction by accepting electrons from the functional group to form silver nanoparticles (Bhakya et al. 2016; Khandel et al. 2018). Alkene and alcohol groups (Fig. 6) present in the CPS extract are responsible for the reduction of the silver ion.

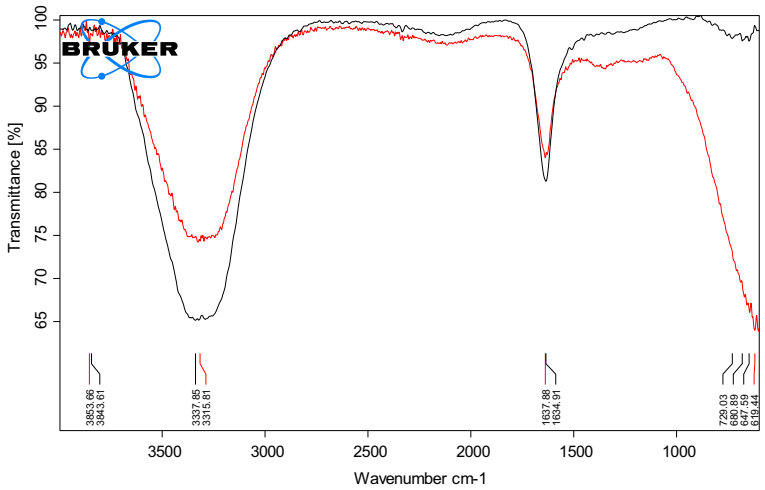

Fig. 6 FTIR spectral band of CPS extract (black color) and biogenic silver nanoparticle (red color)

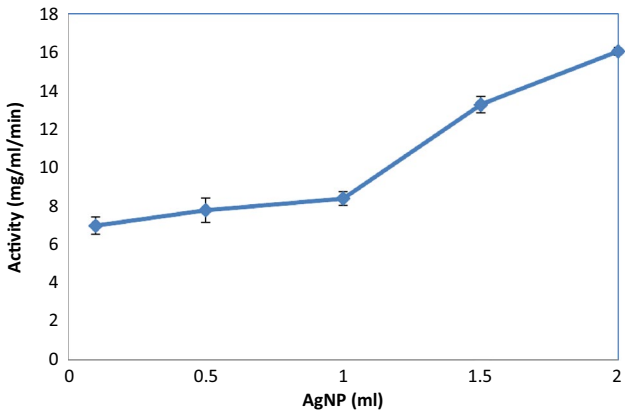

Fig. 7 Effect of biogenic silver nanocatalyst on amylase activity

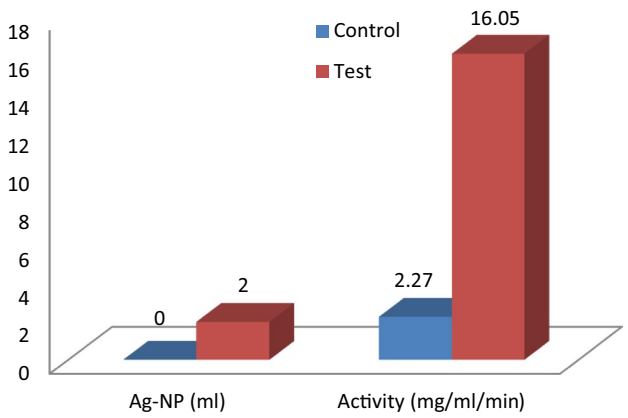

Fig. 8 Comparison of amylase activity with control

Effect of silver nanocatalyst on amylase activity

Herein, it was noticed that the starch hydrolysis process escalated due to the presence of silver nanocatalysts (Fig. 7). Amylase activity was found to increase as the volume of the nanocatalyst increased. The amylase activity of the control (without silver nanocatalyst) was reported to be 2.27 mg/ml/min. In the presence of the catalyst, 16.05 mg/ml/min of enzyme activity was reported (Fig. 8). This signifies that the amylase activity was enhanced by sevenfold when compared to the control. Based on the investigation, it is also evident that silver nanocatalyst has the potential to be used for escalating starch hydrolysis in vitro. Comparatively, the present study justifies well with the studies conducted on silver nanoparticles synthesized using *Piper betel* and *Jatropha curcas* wherein it is reported to enhance the amylase activity by 3 folds (Halima and Narula 2019). Comparison of amylase activity in presence of silver nanoparticle with available report reveals that, larger size silver nanoparticle enhanced the enzyme activity and smaller size nanoparticle inhibited the enzyme activity (Table 1).

Dye degradation

Reduction in the intensity of absorption spectra of MB dye with respect to time proves the progress in degradation. The degradation was completed within 17 min in the presence of silver nanoparticles and $NaBH_4$ (Fig. 9A). In absence of silver nanoparticles, significant degradation was not observed. Electron relay from BH_4^- methylene blue facilitates the degradation. Possibly the excitation of surface electrons and its interaction with dissolved oxygen in the solution along with the production of hydroxyl free radical leads to the significant interaction of silver ions with dye molecules (Vinayagam et al. 2017; Yadav et al. 2019). Biogenic silver nanoparticles absorb methylene blue and $NaBH_4$ on the surface. Methylene blue and $NaBH_4$ act as electrophile and nucleophile respectively. Possible dye degradation mechanisms involve the ability of $NaBH_4$ on electron donation and acceptance capability of methylene

Table 1 Comparison of amylase activity in presence of synthesized silver nanoparticle

SI. No.	Size of silver nanoparticles and source of synthesis	Effect on amylase	References
1.	42 nm (*Jatropha curcas* extract mediated synthesis)	Reaction rate: threefold increase	(Halima and Narula 2019)
2.	5 to 20 nm (*Lentinus tuber-regium* extract mediated synthesis)	Inhibited the amylase activity	(Debnath et al. 2020)
3.	36 nm (chemical fabricated silver nanoparticles)	Activity increased by ninefold	(Krishnakumar et al. 2018)
4.	5 to 40 nm (soluble starch mediated synthesis)	Activity increased by 4.7 fold	(Ernest et al. 2012)
5.	5 to 15 nm (*Bauhinia variegata* flower extract mediated synthesis)	Inhibited the amylase activity	(Johnson et al. 2017)
6.	26.52 nm (*Cannabis sativa* leaf extract mediated synthesis)	Inhibited the activity	(Chouhan and Guleria 2020)
7.	48.83 to 55.24 nm (Cocoa pod shells extract mediated synthesis)	Activity increased by sevenfold	Current work

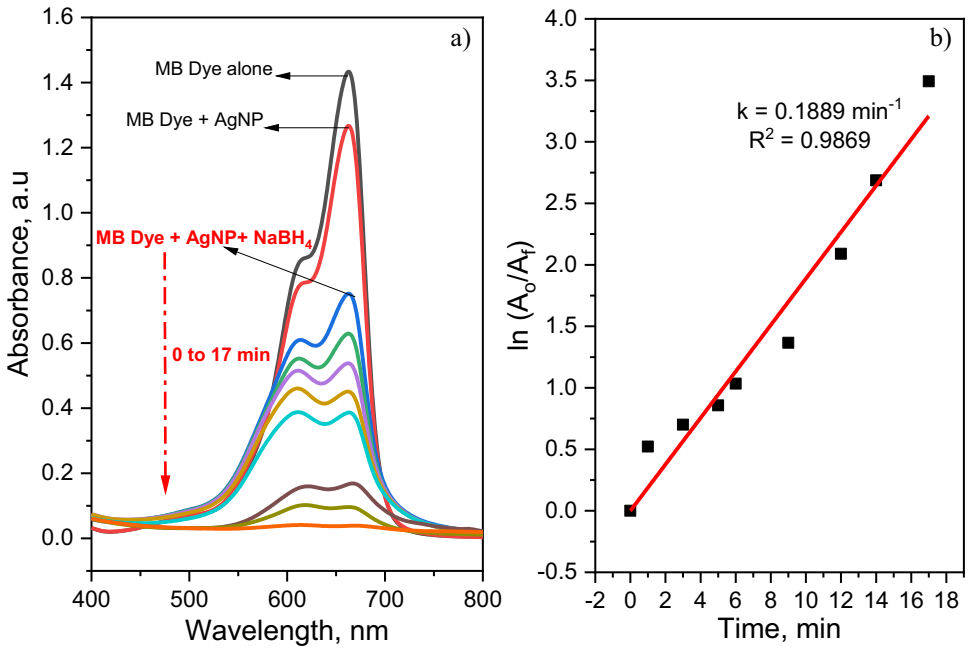

Fig. 9 **A** UV–Vis spectra and **B** First-order degradation kinetics of MB dye in the presence of AgNP and $NaBH_4$

blue dye molecules. Biogenic silver nanoparticles play the role of relay system in a homogeneous reaction process in the transfer of electrons essential for methylene blue dye degradation (Varadavenkatesan et al. 2020a, b; David and Moldovan 2020). Methylene blue will degrade into leucomethyene Blue (Hu et al. 2019). Spontaneously desorbed leucomethyene Blue diffuses into solution. Colorless molecules such as H_2O, SO_4^{-2}, and CO_2 are generated during dye degradation (Moon et al. 2018). The pseudo-first-order reaction model fits well with the degradation of methylene blue dye exhibiting R^2 of 0.9869 and the degradation constant was calculated to be 0.1889 min^{-1} from the plot ln (A_0/A_f) vs time (Fig. 9B). Table 2 provide the comparison of methylene blue dye degradation using silver nanoparticles.

Inhibition activity against FocR4 with silver nanoparticle

The results of biogenic nanoparticles in the present study demonstrated that the zone inhibition was found to be 34% (Fig. 10c) after 5 days of incubation. The crude extract comparatively showed no activity as is visible in Fig. 10b, wherein the FocR4 growth had covered the entire Petri plate within 5 days of incubation. The growth of pure FocR4 culture is depicted in Fig. 10a.

The inhibition mechanism could be possibly the ions that are released by the nanoparticles binding to the few protein groups, which further interfere with the cell permeability. In general, nanoparticles ranging between 10 to 70 nm penetrate the cell membrane causing rupture of the cell walls and releasing the cell contents. Thus, an increase in the size of the nanoparticle makes the regular pattern of growth and development of the fungi almost impossible. In the present study, the size of the nanoparticles ranged between 48.83 to 55.24 nm, which resulted in the appropriate inhibition pattern destroying the conidia thereby disrupting the electron transport, protein oxidation, and membrane potential. These nanoparticles also may be responsible for inducing oxidative stress causing severe protein damage, membrane damage, and nutrient absorption by directly attacking the

Table 2 Comparison of methylene blue degradation using biosynthesized silver nanoparticle

SI No.	Size of the silver nanoparticles	Results	References
1.	31 nm	Absorbance: 0.5 to 0 Time: 14 min % Degradation: 92.06% Pseudo-first-order reaction kinetics	(Huy Tran et al. 2018)
2.	19 nm	Absorbance: 2.0 to 0 Time: 20 min % Degradation: 99.00% Pseudo-first-order reaction kinetics $R^2 = 0.981$	(Somasundaram et al. 2021)
3.	5 to 25 nm	Absorbance: 0.6 to 0.22 Time: 72 h % Degradation: 92.00%	(Al-Zaban et al. 2021)
4.	–	Absorbance: – Time: 08 min % Degradation: 100.00% Pseudo-first-order reaction kinetics	(Khansole 2022)
5.	–	Absorbance: Time: 12 min % Degradation: 99.00% Pseudo-first-order reaction kinetics $R^2 = 0.9477$	(Song et al. 2022)
6.	–	Absorbance: Time: 13 min % Degradation: –	(Bonnia et al. 2016)
7.	–	Absorbance: 3.2 to 0 Time: 80 min % Degradation: Pseudo-first-order reaction kinetics $R^2 = –$	(Chikkanayakanahalli Paramesh et al. 2021)
8.	48.83 to 55.24 nm	Absorbance: 1.2 to 0 Time: 17 min % Degradation: 100 Pseudo-first-order reaction kinetics $R^2 = 0.9869$	Current work

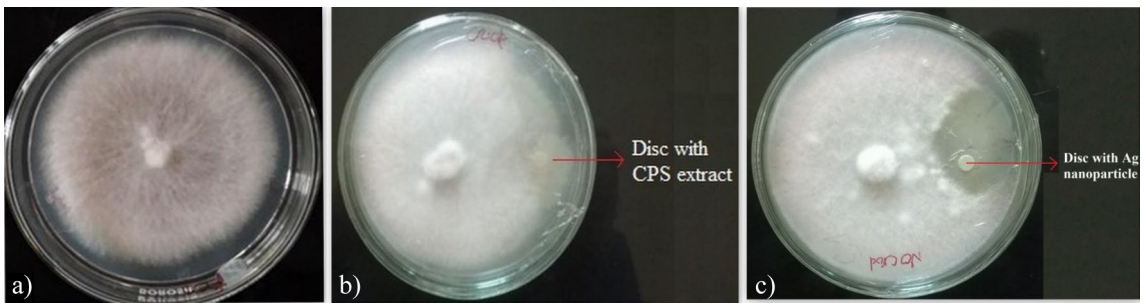

Fig. 10 **a** Growth of *FoCR4*, **b** growth of FocR4 on CPS crude Extract, **c** CPS Ag nanoparticle disc inhibition zone against FocR4

DNA (Cruz-Luna et al. 2021). Silver nanoparticles adhere to fungal hyphae and disrupt the integrity of the fungal cells. Primarily, silver ions interfere with the function of the membrane-bound enzyme, disrupt the replication of DNA, and block the expression of enzymes and proteins (Dawoud et al. 2021).

These results are in good justification with the studies conducted by Pham et al. 2019, wherein using copper nanoparticles in colloidal form has depicted 100% inhibition. Based on the literature survey, this study reports the first of its kind on the inhibition of FocR4 using silver nanoparticles from CPS. Further studies need to be corroborated in this

Table 3 Comparison of antifungal activity of biosynthesized silver nanoparticle against *Fusarium oxysporum*

SI. No.	Size of silver nanoparticles and source of synthesis	Antifungal activity	References
1.	33. 26 nm (silver nanoparticles coated with chitosan)	74% inhibition with 2000 ppm	(Basurto et al. 2020)
2.	(*Satureja hortensis* seeds mediated synthesis)	35% inhibition with 5000 ppm	(Abkhoo and Panjehkeh 2017)
3.	50.6 nm (*Malva parviflora* L. leaf extract mediated synthesis)	80% inhibition	(Al-Otibi et al. 2021)
4.	3 to 13 nm (*Nigrospora oryzae* isolate extract mediated synthesis)	64.16% inhibition	(Dawoud et al. 2021)
5.	48.83 to 55.24 nm (Cocoa pod shells extract mediated synthesis)	34% inhibition	Current work

area which may provide insight into the specificity of these nanoparticles in combating FocR4 and in turn helping the cultivars effectively in the growth of crops. Comparison of antifungal activity against *Fusarium oxysporum* exhibited by biosynthesized nanoparticles is provided in Table 3.

Conclusion

The research encompasses that silver nanoparticle was successfully synthesized using CPS extract. Zeta sizer report revealed the size range of colloidal silver nanoparticles as approximately between 190 to 490 nm with an average hydrodynamic diameter of 384 nm. Significantly, the functional groups like alkene and alcohols present in the CPS extract have transferred to the silver nanoparticle surface during the silver ion reduction process. SEM with EDS and XRD analysis attested to the existence of the silver nanoparticles. SEM analysis indicates the diameter of silver nanoparticles ranging from 48.83 to 55.24 nm. The sharp peak of 33.16° in XRD analysis proves (101) fcc plane and the crystallite size of silver nanoparticles was calculated as 59.65 nm. This work spotlights the enhanced in vitro activity of amylase in presence of silver nanocatalysts explored in the spectra of application in industrial processes. Methylene blue dye was degraded in presence of silver nanoparticles proving the potential nanocatlytic property. The dye degradation process follows a pseudo-first-order reaction model. In addition, the biogenic nanoparticles in the present study have exhibited anti-Foc activity, which proves to hold a promising tool in the future agricultural domain in resolving pest management, wherein this biogenic solution could be suitably applied to the crops in spray form providing a reasonable alternative in an effective and economic form.

Acknowledgement Mr. Anantha Ramakrishna from the Peruvai village of Vittla (Dakshina Kannada district, Karnataka), India provided the cocoa pod shells used in the study.

Declarations

Conflict of interest On behalf of all authors, the corresponding author states that there is no conflict of interest.

Ethical approval Not applicable.

References

Abkhoo J, Panjehkeh N (2017) Evaluation of antifungal activity of silver nanoparticles on fusarium oxysporum. Int J Infect. https://doi.org/10.5812/IJI.41126

Ahmed HE, Kolisis FN (2011) An investigation into the removal of starch paste adhesives from historical textiles by using the enzyme α-amylase. J Cult Herit 12:169–179. https://doi.org/10.1016/j.culher.2010.08.001

Al-Buriahi AK, Al-shaibani MM, Mohamed RMSR et al (2022) Ciprofloxacin removal from non-clinical environment: a critical review of current methods and future trend prospects. J Water Process Eng 47:102725. https://doi.org/10.1016/J.JWPE.2022.102725

Al-Otibi F, Perveen K, Al-Saif NA et al (2021) Biosynthesis of silver nanoparticles using *Malva parviflora* and their antifungal activity. Saudi J Biol Sci 28:2229–2235. https://doi.org/10.1016/J.SJBS.2021.01.012

Al-Zaban MI, Mahmoud MA, AlHarbi MA (2021) Catalytic degradation of methylene blue using silver nanoparticles synthesized by honey. Saudi J Biol Sci 28:2007–2013. https://doi.org/10.1016/J.SJBS.2021.01.003

Anchan S, Pai S, Sridevi H et al (2019) Biogenic synthesis of ferric oxide nanoparticles using the leaf extract of Peltophorum pterocarpum and their catalytic dye degradation potential. Biocatal Agric Biotechnol 20:101251. https://doi.org/10.1016/j.bcab.2019.101251

Assad H, Kaya S, Senthil Kumar P et al (2022) Insights into the role of nanotechnology on the performance of biofuel cells and the production of viable biofuels: a review. Fuel 323:124277. https://doi.org/10.1016/J.FUEL.2022.124277

Basurto DAE, Carvajal FA, Calderon AA et al (2020) Nanopartículas de plata recubiertas con quitosano contra la marchitez vascular causada por *Fusarium oxysporum* en plantúlas de tomate. Biotecnia 22:73–80. https://doi.org/10.18633/BIOTECNIA.V22I3.952

Bhakya S, Muthukrishnan S, Sukumaran M, Muthukumar M (2016) Biogenic synthesis of silver nanoparticles and their antioxidant and antibacterial activity. Appl Nanosci 6:755–766. https://doi.org/10.1007/S13204-015-0473-Z/FIGURES/9

Bonnia NN, Kamaruddin MS, Nawawi MH et al (2016) Green biosynthesis of silver nanoparticles using 'polygonum hydropiper' and study its catalytic degradation of methylene blue. Procedia Chem 19:594–602. https://doi.org/10.1016/J.PROCHE.2016.03.058

Chikkanayakanahalli Paramesh C, Halligudra G, Gangaraju V et al (2021) Silver nanoparticles synthesized using saponin extract of Simarouba glauca oil seed meal as effective, recoverable and reusable catalyst for reduction of organic dyes. Result Surf Interfaces 3:100005. https://doi.org/10.1016/J.RSURFI.2021.100005

Chouhan S, Guleria S (2020) Green synthesis of AgNPs using Cannabis sativa leaf extract: characterization, antibacterial, anti-yeast and α-amylase inhibitory activity. Mater Sci Energy Technol 3:536–544. https://doi.org/10.1016/J.MSET.2020.05.004

Cruz G, Pirilä M, Huuhtanen M et al (2012) Production of activated carbon from cocoa (*Theobroma cacao*) Pod Husk. J Civil Environ Eng. https://doi.org/10.4172/2165-784X.1000109

Cruz-Luna AR, Cruz-Martínez H, Vásquez-López A, Medina DI (2021) Metal nanoparticles as novel antifungal agents for sustainable agriculture: current advances and future directions. J Fungi 7:1033. https://doi.org/10.3390/JOF7121033

da Maia JL, Cardoso JS, da Silveira Mastrantonio DJ et al (2020) Microalgae starch: a promising raw material for the bioethanol production. Int J Biol Macromol 165:2739–2749

David L, Moldovan B (2020) Green synthesis of biogenic silver nanoparticles for efficient catalytic removal of harmful organic dyes. Nanomater (basel, Switzerland). https://doi.org/10.3390/NANO10020202

Dawoud TM, Yassin MA, El-Samawaty ARM, Elgorban AM (2021) Silver nanoparticles synthesized by *Nigrospora oryzae* showed antifungal activity. Saudi J Biol Sci 28:1847–1852. https://doi.org/10.1016/J.SJBS.2020.12.036

Debnath G, Das P, Saha AK (2020) Characterization, antimicrobial and α-amylase inhibitory activity of silver nanoparticles synthesized by using mushroom extract of lentinus tuber-regium. Proc Natl Acad Sci India Sect B - Biol Sci 90:37–45. https://doi.org/10.1007/S40011-019-01076-Y/METRICS

Dewi VS, Chusniasih D, Tutik T (2021) Identification phytochemical compound of ethanol and acetone extract of Cocoa Pods (*Theobroma cacao* L.) using GC-MS You may also like Cocoa clone resistance to phytophthora pod rot (PPR) and Cocoa pod borer (CPB) in South Sulawesi. J Phys Conf Ser 1882:12103. https://doi.org/10.1088/1742-6596/1882/1/012103

Dhyani A (2016) Preparation and characterization of atenolol laden nanoparticles. J Nanomed Res. https://doi.org/10.15406/jnmr.2016.04.00084

Dita M, Barquero M, Heck D et al (2018) Fusarium wilt of banana: current knowledge on epidemiology and research needs toward sustainable disease management. Front Plant Sci 871:1468. https://doi.org/10.3389/FPLS.2018.01468/BIBTEX

Ernest V, Shiny PJ, Mukherjee A, Chandrasekaran N (2012) Silver nanoparticles: a potential nanocatalyst for the rapid degradation of starch hydrolysis by α-amylase. Carbohydr Res 352:60–64. https://doi.org/10.1016/J.CARRES.2012.02.009

Falkowska M, Molga EJ (2014) Nanosilver: a catalyst in enzymatic hydrolysis of starch. Polish J Chem Technol 16:111–113. https://doi.org/10.2478/pjct-2014-0060

Halima R, Narula A (2019) Green synthesis and optimization of silver nanoparticles from Piper betel and Jatropha curcas to enhance α-amylase activity. Asian J Chem 31:2969–2975. https://doi.org/10.14233/ajchem.2019.22269

Hao E, Schatz GC, Hupp JT (2004) Synthesis and optical properties of anisotropic metal nanoparticles. J Fluoresc 14:331–341

Hu M, Yan X, Hu X et al (2019) Synthesis of silver decorated silica nanoparticles with rough surfaces as adsorbent and catalyst for methylene blue removal. J Sol-Gel Sci Technol 89:754–763. https://doi.org/10.1007/S10971-018-4871-Z/TABLES/4

Huy Tran Q, Quy Nguyen V, Le A-T et al (2018) Degradation of methylene blue using silver nanoparticles synthesized from imperata cylindrica aqueous extract. IOP Conf Ser Earth Environ Sci 105:012018. https://doi.org/10.1088/1755-1315/105/1/012018

Ider M, Abderrafi K, Eddahbi A et al (2017) Silver metallic nanoparticles with surface plasmon resonance: synthesis and characterizations. J Clust Sci 28:1051–1069. https://doi.org/10.1007/s10876-016-1080-1

Jain PK, Soni A, Jain P, Bhawsar J (2016) Phytochemical analysis of Mentha spicata plant extract using UV-VIS, FTIR and GC/MS technique. J Chem Pharm Res 8:1–6

Johnson P, Krishnan V, Loganathan C et al (2017) Rapid biosynthesis of Bauhinia variegata flower extract-mediated silver nanoparticles: an effective antioxidant scavenger and α-amylase inhibitor. Artif Cells Nanomed Biotechnol 46:1488–1494. https://doi.org/10.1080/21691401.2017.1374283

Khandel P, Yadaw RK, Soni DK et al (2018) Biogenesis of metal nanoparticles and their pharmacological applications: present status and application prospects. J Nanostruct Chem 83(8):217–254. https://doi.org/10.1007/S40097-018-0267-4

Khansole SV (2022) Study on catalytic reduction of methylene blue using silver nanoparticles synthesized via green route. IJRASET. https://doi.org/10.22214/ijraset.2022.46942

Krishnakumar S, Janani P, Mugilarasi S et al (2018) Chemical induced fabrication of silver nanoparticles (Ag-NPs) as nanocatalyst with alpha amylase enzyme for enhanced breakdown of starch. Biocatal Agric Biotechnol 15:377–383. https://doi.org/10.1016/j.bcab.2018.06.016

Lateef A, Ojo SA, Akinwale AS et al (2015) Biogenic synthesis of silver nanoparticles using cell-free extract of *Bacillus safensis* LAU 13: antimicrobial, free radical scavenging and larvicidal activities. Biol 70:1295–1306. https://doi.org/10.1515/biolog-2015-0164

Miller GL (1959) Use of dinitrosalicylic acid reagent for determination of reducing sugar. Anal Chem 31:426–428. https://doi.org/10.1021/ac60147a030

Monroy Y, Seré P, Rivero S, García MA (2020) Sustainable panels based on starch bioadhesives: an insight into structural and tribological performance. Int J Biol Macromol 148:898–907. https://doi.org/10.1016/j.ijbiomac.2020.01.205

Moon SA, Salunke BK, Saha P et al (2018) Comparison of dye degradation potential of biosynthesized copper oxide, manganese dioxide, and silver nanoparticles using Kalopanax pictus plant extract. Korean J Chem Eng 35:702–708. https://doi.org/10.1007/S11814-017-0318-4/METRICS

Nandiyanto ABD, Oktiani R, Ragadhita R (2019) How to read and interpret ftir spectroscope of organic material. Indones J Sci Technol 4:97–118. https://doi.org/10.17509/ijost.v4i1.15806

Nguyen PA, Nguyen AVP, Dang-Bao T et al (2020) Green synthesis of copper nanoparticles using Cocoa pod extract and its catalytic activity in deep oxidation of aromatic hydrocarbons. SN Appl Sci 2:1–13. https://doi.org/10.1007/S42452-020-03539-8/FIGURES/15

Pai S, Sridevi H, Varadavenkatesan T et al (2019) Photocatalytic zinc oxide nanoparticles synthesis using Peltophorum pterocarpum leaf extract and their characterization. Optik (stuttg) 185:248–255. https://doi.org/10.1016/j.ijleo.2019.03.101

Pham ND, Duong MM, Le MV et al (2019) Preparation and characterization of antifungal colloidal copper nanoparticles and their antifungal activity against Fusarium oxysporum and Phytophthora capsici. Comptes Rendus Chim 22:786–793. https://doi.org/10.1016/j.crci.2019.10.007

Raja S, Ramesh V, Thivaharan V (2015) Antibacterial and anticoagulant activity of silver nanoparticles synthesised from a novel source–pods of Peltophorum pterocarpum. J Ind Eng Chem 29:257–264. https://doi.org/10.1016/j.jiec.2015.03.033

Shet VB, Sanil N, Bhat M et al (2018) Acid hydrolysis optimization of cocoa pod shell using response surface methodology approach toward ethanol production. Agric Nat Resour 52:581–587. https://doi.org/10.1016/j.anres.2018.11.022

Shet VB, Rakshith KG, Shetty NJ et al (2019) The application of response surface methodology for the optimization of autoclave assisted hcl hydrolysis of an agro residue cocoa pod shells for releasing reduced sugars. J Microbiol Biotechnol Food Sci 9:548–551. https://doi.org/10.15414/jmbfs.2019/20.9.3.548-551

Somasundaram CK, Atchudan R, Edison TNJI et al (2021) Sustainable synthesis of silver nanoparticles using marine algae for catalytic degradation of methylene blue. Catalysts 11:1377. https://doi.org/10.3390/CATAL11111377/S1

Song WC, Kim B, Park SY et al (2022) Biosynthesis of silver and gold nanoparticles using Sargassum horneri extract as catalyst for industrial dye degradation. Arab J Chem 15:104056. https://doi.org/10.1016/J.ARABJC.2022.104056

Thakur A, Kumar A, Kaya S et al (2022) Suppressing inhibitory compounds by nanomaterials for highly efficient biofuel production: a review. Fuel 312:122934. https://doi.org/10.1016/J.FUEL.2021.122934

Tong Z, Tong Y, Shi YC (2019) Partial swelling of granules enables high conversion of normal maize starch to glucose catalyzed by granular starch hydrolyzing enzyme. Ind Crops Prod 140:111626. https://doi.org/10.1016/j.indcrop.2019.111626

Varadavenkatesan T, Selvaraj R, Vinayagam R (2020a) Green synthesis of silver nanoparticles using Thunbergia grandiflora flower extract and its catalytic action in reduction of Congo red dye. Mater Today Proc 23:39–42. https://doi.org/10.1016/j.matpr.2019.05.441

Varadavenkatesan T, Vinayagam R, Selvaraj R (2020b) Green synthesis and structural characterization of silver nanoparticles synthesized using the pod extract of Clitoria ternatea and its application towards dye degradation. Mater Today Proc 23:27–29. https://doi.org/10.1016/j.matpr.2019.04.216

Varadavenkatesan T, Pai S, Vinayagam R, Selvaraj R (2021) Characterization of silver nano-spheres synthesized using the extract of *Arachis hypogaea* nuts and their catalytic potential to degrade dyes. Mater Chem Phys 272:125017. https://doi.org/10.1016/j.matchemphys.2021.125017

Vinayagam R, Varadavenkatesan T, Selvaraj R (2017) Evaluation of the anticoagulant and catalytic activities of the bridelia retusa fruit extract-functionalized silver nanoparticles. J Clust Sci 285(28):2919–2932. https://doi.org/10.1007/S10876-017-1270-5

Vinayagam R, Varadavenkatesan T, Selvaraj R (2018) Green synthesis, structural characterization, and catalytic activity of silver nanoparticles stabilized with *Bridelia retusa* leaf extract. Green Process Synth 7:30–37. https://doi.org/10.1515/gps-2016-0236

Vo CM, Cao ANT, Saleh Qazaq A et al (2022) Toward syngas production from simulated biogas dry reforming: promotional effect of calcium on cobalt-based catalysts performance. Fuel 326:125106. https://doi.org/10.1016/J.FUEL.2022.125106

Wang D, Ma X, Yan L et al (2017) Ultrasound assisted enzymatic hydrolysis of starch catalyzed by glucoamylase: investigation on starch properties and degradation kinetics. Carbohydr Polym 175:47–54. https://doi.org/10.1016/j.carbpol.2017.06.093

Yadav P, Manjunath H, Selvaraj R (2019) Antibacterial and dye degradation potential of zero-valent silver nanoparticles synthesised using the leaf extract of Spondias dulcis. IET Nanobiotechnol 13:84–89. https://doi.org/10.1049/IET-NBT.2018.5058

Yadav K, Damodaran T, Dutt K et al (2021) Effective biocontrol of banana fusarium wilt tropical race 4 by a bacillus rhizobacteria strain with antagonistic secondary metabolites. Rhizosphere 18:100341. https://doi.org/10.1016/J.RHISPH.2021.100341

Publisher's Note Springer Nature remains neutral with regard to jurisdictional claims in published maps and institutional affiliations.

Springer Nature or its licensor (e.g. a society or other partner) holds exclusive rights to this article under a publishing agreement with the author(s) or other rightsholder(s); author self-archiving of the accepted manuscript version of this article is solely governed by the terms of such publishing agreement and applicable law.